Thermochimica Acta 510 (2010) 97–102

Contents lists available at ScienceDirect

Thermochimica Acta

journal homepage: www.elsevier.com/locate/tca

Thermal properties of poly(L-lactide)/olive stone flour composites

Sanja Perinović*, Branka Andričić, Matko Erceg

Department of Organic Technology, Faculty of Chemistry and Technology, University of Split, Teslina 10/V, 21000 Split, Croatia

ARTICLE INFO

Article history:
Received 20 April 2010
Received in revised form 1 July 2010
Accepted 2 July 2010
Available online 21 August 2010

Keywords:
Poly(L-lactide) (PLLA)/olive stone flour (OSF) composites
Differential scanning calorimetry (DSC)
Scanning electron microscopy (SEM)
Thermogravimetric analysis (TGA)
Activation energy (E_a)

ABSTRACT

Thermal properties of poly(L-lactide)/olive stone flour (PLLA/OSF) composites were investigated by differential scanning calorimetry (DSC) and thermogravimetric analysis (TGA) using dynamic heating regime. PLLA was blended with various amount of OSF using Brabender plastograph and pressed in a hydraulic hot press. DSC analysis showed that the glass transition temperature and the melting temperature of PLLA in the composites remained the same, while the cold crystallization temperature decreased. The crystallinity of PLLA was changed, too. SEM analysis confirmed weak interactions between polymer matrix and the filler. According to TG analysis, PLLA decomposes in one step, PLLA/OSF composites in two and OSF in three degradation steps. As the amount of OSF increases, thermal stability of PLLA decreases. At conversion higher than 0.7 char formation is probably responsible for higher E_a values of nonisothermal degradation of PLLA composites compared to pure PLLA.

1. Introduction

Exhaustion of petroleum resources and global pollution of environment force society to establish new environmental regulations and create new materials from renewable resources that will assure sustainable development. One of those eco-friendly materials is poly(L-lactide) (PLLA) whose waste can be treated by different waste management procedures and consequently its natural cycle can be closed. PLLA is a biodegradable polymer synthesized from lactic acid produced by fermentation of sugar or starch feedstock like potato, corn, wheat, sugarcane etc [1]. Although these are renewable resources they have to be used very carefully not to jeopardise the basic needs for food. Furthermore, PLLA is brittle thermoplastic aliphatic polyester with relatively good mechanical properties similar to polystyrene [1]. PLLA is very attractive and useful polyester, synthesized in 1960s and probably the high interest for it will continue. The main reason for this is variety of applications after modification of its properties. Compared to commercial polymers PLLA is still too expensive and adding an adequate filler is the easiest way to reduce its costs and at the same time improve or at least hold the properties of the starting material.

In the Mediterranean region of Croatia olives are of great agricultural importance as a source of olive oil. Olive stones, as the by-products of olive oil production are very interesting for further use, both from economical and environmental point of view. Olive stone flour (OSF) is produced simply by milling olive stones. It is composed of cellulose, hemicellulose, lignin, water, some fat, proteins and free sugars [2]. Lignocellulosic materials have a lot of positive features, such as low density, low requirements on processing equipment, no abrasion during processing, abundance and biodegradability [3]. Therefore, OSF can be incorporated into PLLA as organic filler to reduce costs and improve mechanical properties of the composite material. In this way a fully biodegradable material can be produced. It was also proved that reinforcing PLLA with different fibers, is the one of the possibilities to improve its thermal stability [4].

PLLA has poor thermal stability and its thermal degradation is mainly caused by intra- and inter-molecular transesterification reactions leading to cyclic oligomers of lactic acid and lactide [5–10]. Mechanism of the pyrolysis of OSF (i.e. cellulose, hemicellulose and lignin) is not clear due to the chemical differences from species to species and complexity of reactions during pyrolysis [11]. It is also important to know how PLLA/OSF composites will behave during processing or application. Many researchers have investigated the thermal properties of PLLA, but there is no information on the thermal properties of PLLA/OSF composites. To predict the thermal behaviour of PLLA/OSF composites outside the experimental region it is necessary to perform kinetic analysis, in the first place to get information about activation energy (E_a). Hence, kinetic prediction can be easily accomplished using E_a evaluated by isoconversional methods which are considered as the most reliable method for the calculation of E_a and E_a-conversion (α) dependence of thermally activated reactions [12,13]. From E_a-α dependence it is possible to get a clue about complexity of a process and to identify its kinetic scheme [13]. The objective of the present investigations is to study the effects of different amounts of OSF on the thermal

* Corresponding author. Tel.: +385 21 329 455; fax: +385 21 329 461.
E-mail address: sanja@ktf-split.hr (S. Perinović).

0040-6031/$ – see front matter © 2010 Elsevier B.V. All rights reserved.
doi:10.1016/j.tca.2010.07.002

Table 1
Characteristics of used OSF.

Loss on drying (%)	10
Bulk density (g dm^{-3})	570
pH-value	6
Residue on ignition (%)	1
Colour	Brown
Composition	Cellulose, Hemicellulose and Lignine (~90%) Water (~10%)

Table 2
Composition of PLLA/OSF composites.

Sample	PLLA/weight parts	OSF/weight parts
PLLA	100	0
PLLA 10	100	10
PLLA 20	100	20
PLLA 30	100	30

properties and thermal stability of PLLA by differential scanning calorimetry and thermogravimetric analysis.

2. Experimental

2.1. Materials

Poly(L-lactide) (PLLA), Biomer L9000, in pellet form was obtained from Biomer (Germany), $\overline{M_v} \approx 58700$ ($[\eta]_{25\,^\circ C} = 165\,cm^3\,g^{-1}$ in chloroform) [14]. Olive stone flour (OSF), Jeluxyl OM 3000, was purchased from Jelu-Werk (Germany). OSF as received was additionally sieved to obtain finer particles, from 50 to 150 mesh size. PLLA pellets and OSF were dried in a vented oven at 100 °C for 8 h prior to processing to remove moisture. The characteristics of the filler are listed in Table 1.

2.2. Sample preparation

PLLA was blended with various amounts of OSF, as shown in Table 2, using Brabender plastograph operating at 170 °C for 3 min at 70 rpm. Pure PLLA and PLLA/OSF composite samples were then removed from the plastograph as small clumps and moulded at 175 °C for 3 min in a hydraulic hot press. After moulding samples where cooled down between thick metal blocks at a room temperature and the plates of 35 mm × 15 mm × 1 mm were obtained.

2.3. DSC analysis

The thermal characteristics of the composites were determined using differential scanning calorimeter (DSC 823^e, Mettler-Toledo), equipped with an intracooler. The measurements were performed in the closed aluminium pans under nitrogen atmosphere (flow rate was 30 cm^3 min^{-1}). Approx. 20 mg samples were heated from −50 °C to 200 °C at 10 °C min^{-1} (first heating scan), than cooled from 200 °C to −50 °C at 20 °C min^{-1} (cooling scan) and finally heated from −50 °C to 200 °C at 20 °C min^{-1} (second heating scan). The cold crystallization temperature (T_{cc}) and the melting temperature (T_m) were taken as the peak temperature of the cold crystallization exotherm and the melting endotherm, respectively, whereas the glass transition temperature (T_g) was taken as the inflection point of the specific heat decrement at the glass transition.

2.4. SEM analysis

Bulk morphology of the fractured surfaces was examined using scanning electron microscope (SEM, Tescan) operated at 20 kV. Prior to analysis, the samples were coated with graphite to avoid sample charging under the electron beam.

2.5. TG analysis

The thermal degradation of the composites was investigated thermogravimetrically (Pyris 1 TGA, Perkin-Elmer). Sample mass was 5.0 ± 0.1 mg. TG analysis was carried out in the temperature range from 50 to 500 °C under nitrogen atmosphere (flow rate was 20 cm^3 min^{-1}) at the heating rates of 2.5, 5, 10 and 20 °C min^{-1}.

3. Theory

3.1. Nonisothermal kinetics analysis

Due to the fact that polymer degradation usually includes complex reactions, the variation of activation energy with the extent of conversion is expected. To evaluate the activation energy isoconversional methods have been widely used. Generally, isoconversional methods are based on combination of single-step kinetic equation and Arrhenius equation, Eq. (1):

$$\frac{d\alpha}{dt} = A \exp\left(\frac{-E_a}{RT}\right) f(\alpha) \quad (1)$$

where α is the conversion degree, t is the time, A and E_a are Arrhenius parameters, the preexponential factor and the activation energy, respectively. $f(\alpha)$ is a reaction model and together with A and E makes the kinetic triplet. R is the gas constant and T is the absolute temperature.

Activation energy from nonisothermal data can be calculated according Friedman differential isoconversional method [15] based on Eq. (2):

$$\ln\left[\beta_i \left(\frac{d\alpha}{dT}\right)_{\alpha,i}\right] = \ln[A_\alpha f(\alpha)_i] - \frac{E_{a,\alpha}}{RT_{\alpha,i}} \quad (2)$$

where β is the linear heating rate and $\beta(d\alpha/dT)$ is the rate of reaction, while subscripts i and α designate heating rate and conversion degree, respectively. For any α = constant, the plot $\ln[\beta(d\alpha/dT)]$ versus $1/T$ gives a straight line whose slope is used to evaluate the activation energy.

4. Results and discussion

4.1. DSC analysis

DSC was used to study the thermal properties of pure PLLA and PLLA/OSF composites. The curves obtained from the heating and the cooling scans are shown in Figs. 1–3. The values of the thermal characteristics obtained from DSC curves are presented in Table 3. From the first heating scan the cold crystallization and melting data were obtained while the glass transition was obtained from the second heating scan. From DSC curves and data reported in Table 3 is evident that pure PLLA and its composites are semicrystalline.

X_c of PLLA was calculated according the Eq. (3) [16]:

$$X_c(\%) = \frac{\Delta H_m + \sum \Delta H_{cc}}{\Delta H_{100\%} \times w_{PLLA}} \quad (3)$$

where $\Delta H_{100\%}$ is the melting enthalpy of 100% crystalline PLLA (93 J g^{-1}) and w is the weight fraction of PLLA in the sample.

DSC curves of all samples (Fig. 1) show an exothermic peak of the cold crystallization. T_{cc} of pure PLLA is at 113 °C, but for the

Table 3
Thermal characteristic of PLLA and PLLA/OSF composites.

Sample	T_g (°C)	Δc_p (J g^{-1} °C^{-1})	T_{cc} (°C)	ΔH_{cc} (J g^{-1})	T_m (°C)	ΔH_m (J g^{-1})	X_c (%)
PLLA	63	0.37	113	−23.6	172	26.0	3
PLLA 10	62	0.33	108	−12.3	171	23.9	14
PLLA 20	62	0.31	106	−15.5	171	21.1	8
PLLA 30	62	0.28	107	−19.3	172	20.7	2

Δc_p, specific heat capacity; ΔH_{cc}, cold crystallization enthalpy; ΔH_m, melting enthalpy; X_c, degree of crystallinity.

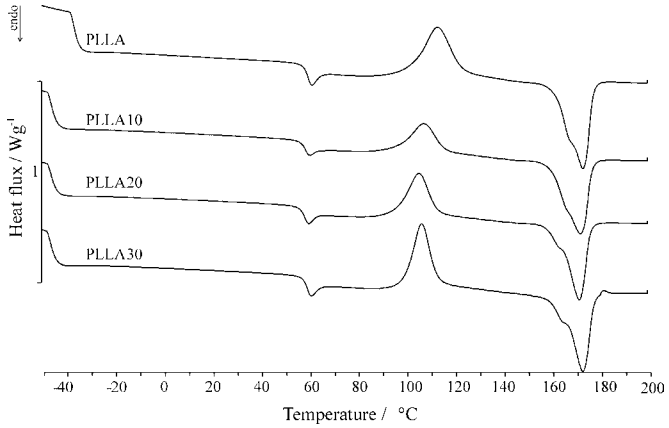

Fig. 1. DSC curves of the first heating scan for PLLA and PLLA/OSF composites.

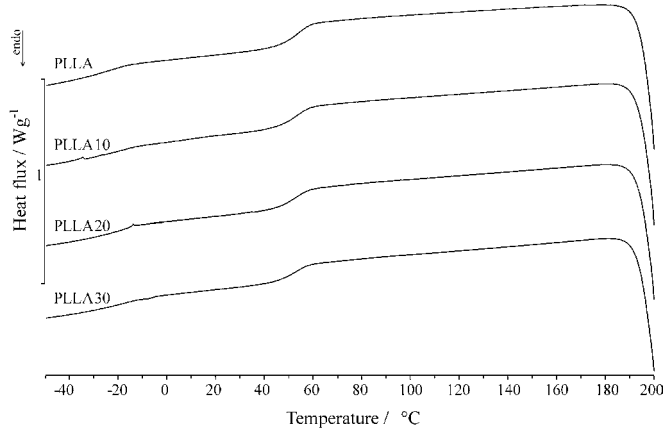

Fig. 2. DSC curves of the cooling scan for PLLA and PLLA/OSF composites.

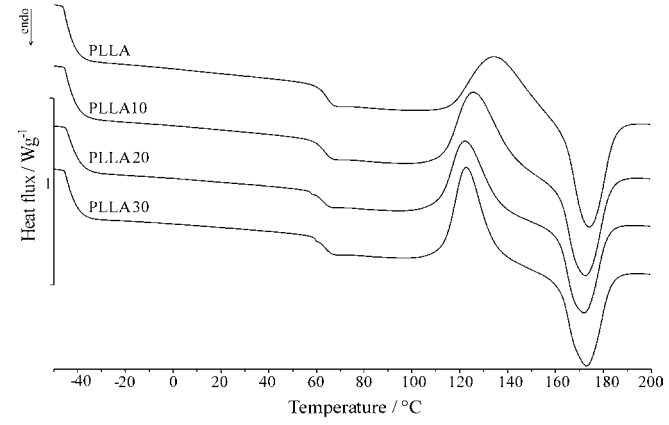

Fig. 3. DSC curves of the second heating scan for PLLA and PLLA/OSF composites.

composites T_{cc} is around 107 °C. OSF decreases T_{cc} of PLLA, but its amount has no significant influence on T_{cc}. In fact, the presence of filler can promote the initial cold crystallization of PLLA matrix [17] and T_{cc} depression is an indication of the nucleating ability of filler [4]. Addition of OSF narrows the crystallization peak and it is narrower as OSF amount increases. Some interesting behaviour is observed for ΔH_{cc}. The absolute value of ΔH_{cc} for pure PLLA is 23.61 J g^{-1} and the absolute values of ΔH_{cc} for the composites are lower, inversely proportional to the filler content. The pre-melting crystallization peak, generally observed for PLLA, was not observed neither for pure PLLA or PLLA/OSF composites. The melting peak of pure PLLA is at 172 °C and PLLA/OSF composites melt at about the same temperature. The melting endotherms are bimodal, i.e. a small shoulder on the melting endotherm of all samples is visible. For pure PLLA this shoulder is around 168 °C, while for PLLA 10, PLLA 20 and PLLA 30 is around 166 °C, 163 °C and 164 °C, respectively. This could be the indication that more than one crystallographic form or morphology change is present during heating. Obviously, addition of OSF has influence on these changes because the shoulder is more pronounced with higher OSF content and shifted towards lower temperatures. ΔH_m of pure PLLA is 26.01 J g^{-1} and it decreases as OSF amount increases. At lower OSF content the crystallization of PLLA (Table 3) was enhanced. OSF acts as a nucleating agent like some other fillers [17]. It was also found by other authors that lignin (one of the components of OSF) in a wood fibers act as a nucleating agent [4]. Also, as OSF amount increases the crystallinity of PLLA starts to decrease from 14 to 2%. It is assumed that this behaviour is not only a consequence of OSF addition but the processing procedure as well, since PLLA granules as received have degree of crystallinity of 49% [18]. The samples were prepared using Brabender plastograph, moulded in a hydraulic hot press and than cooled down between thick metal blocks at room temperature, as described previously. The fast cooling generally lowers crystallinity. The curves in Fig. 2 show that cooling of pure PLLA and PLLA/OSF composites at cooling rate 20 °C min^{-1} does not enable crystallization from the melt. This cooling rate was high enough to prevent the crystallization of PLLA with and without OSF and it can support the presumption about influence of the processing procedure. It is also possible that during processing OSF acts as a nucleation agent and at a same time as an obstacle for polymer chains to make crystals. Therefore, the observed crystallization degree of PLLA/OSF composites is the result of these two opposite influences. At lower content OSF acts as a nucleation agent, but at higher content OSF prevents crystallization because in such environment the motions of PLLA molecules are somewhat limited. PLLA starts to crystallize during next heating as clearly visible in Fig. 3. In those conditions the OSF role as the nucleating agent is present, too. OSF has no influence on glass transition of PLLA suggesting that there are no interactions between polymer matrix and the filler or that they are negligible weak.

4.2. SEM analysis

Fig. 4 shows the micrographs of PLLA composites with different weight parts of OSF. The samples were broken down to analyse the

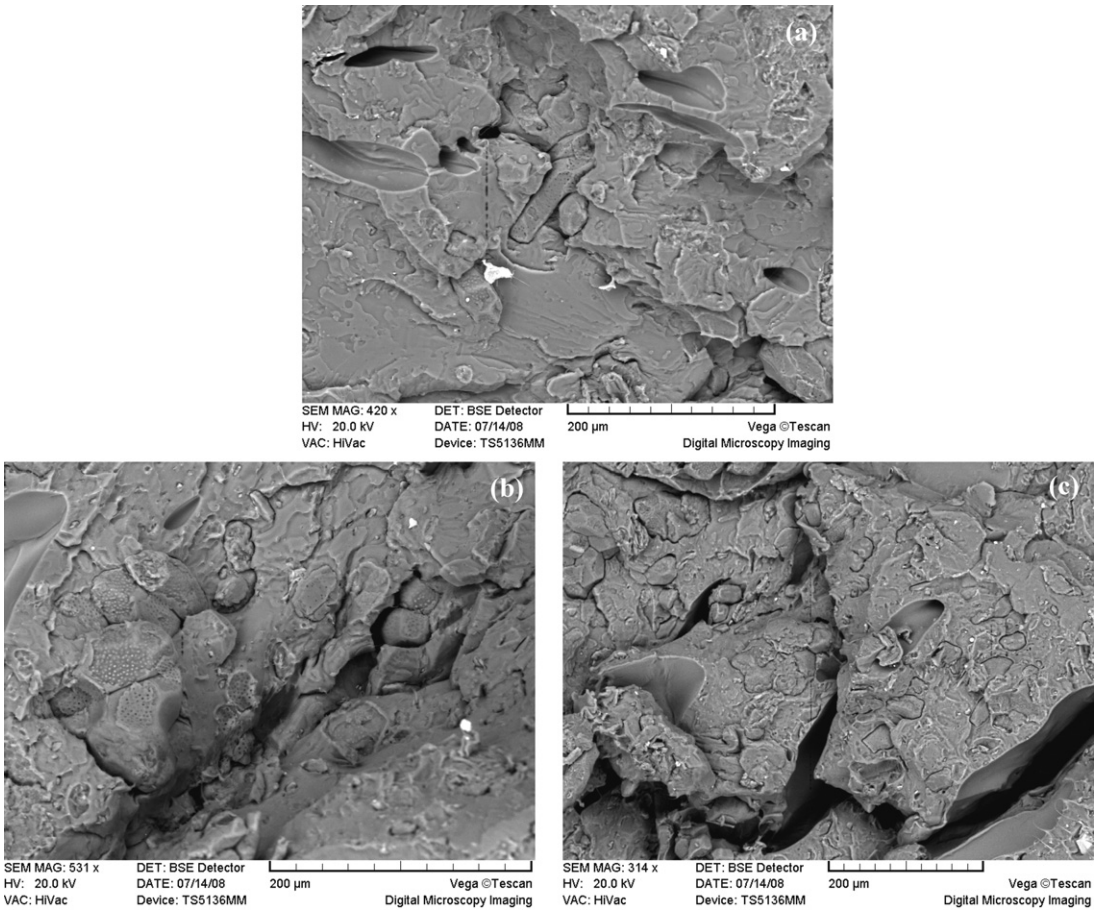

Fig. 4. SEM images of PLLA/OSF composites: (a) PLLA 10; (b) PLLA 20; (c) PLLA 30.

bulk morphology. DSC analysis has already indicated that interactions of OSF with PLLA are weak so SEM images could prove this statement. The OSF is not dispersed equally in PLLA matrix and the agglomerations of OSF are visible. The boundary between OSF and PLLA is sharp as the result of poor wetting of the filler by the polymer. Also, cavities or holes can be seen. All that proves low interfacial adhesion between OSF and PLLA. As the amount of OSF increases the voids and agglomerates are more visible. Particles of OSF were between 50 and 150 mesh size and it is reasonably to expect that small and surface modified particles could provide better dispersion and better interaction with polymer matrix.

4.3. TG analysis

Thermal stability of PLLA is very important since during processing it is exposed to the temperatures above its melting point and degradation could occur. If the system is even more complex, such as the polymer/lignocelulosic filler composite, thermal stability has to be well known, not just for the processing purposes but also for the final application. TG and DTG (derivative TG) curves of pure PLLA, OSF and PLLA/OSF composites degradation at heating rate of 10 °C min^{-1} are presented in Figs. 5 and 6, respectively. Also, TG and DTG curves of thermal degradation for all samples at heating rates of 2.5, 5 and 20 °C min^{-1} were recorded because the measurements at several heating rates, instead at the single one, are necessary to obtain reliable kinetic data. Generally, pure PLLA decomposes fast and completely in one stage above 300 °C at all heating rates. TG curves at heating rates of 2.5 and 5 °C min^{-1} show that except this major degradation stage pure PLLA has a slight weight loss at a beginning of degradation and that DTG curves have visible small shoulders at about 300 °C, depending on the heating rate. These shoulders are also visible at Fig. 6 but they are more pronounced at low heating rates. This is also observed by other authors who concluded that thermal degradation at about 300 °C might be attributed to the aluminium-catalyzed depolymerization due to the residual aluminium catalysts in PLA sample [19]. The main degradation products of PLLA are oligomers together with some lactide, but there are also other volatile products such as acetaldehyde, carbon dioxide, carbon monoxide and ketene [20,21]. On the other hand, OSF starts to decompose above 200 °C and in a broad temperature range. At 500 °C the carbonaceous residue is about 30%. The early

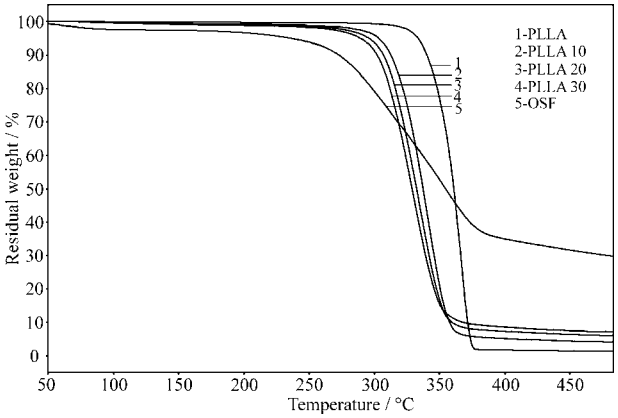

Fig. 5. TG curves of PLLA, OSF and PLLA/OSF composites thermal degradation at heating rate of 10 °C min^{-1}.

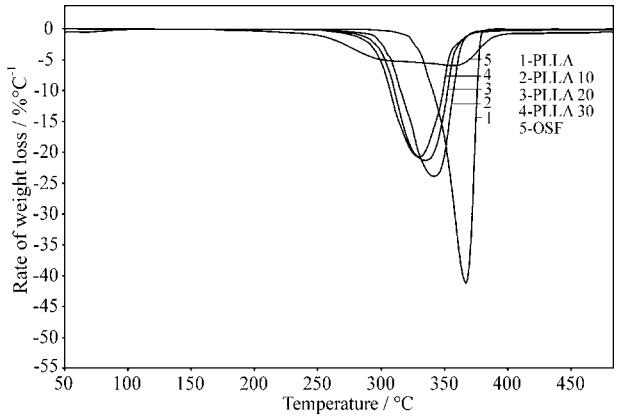

Fig. 6. DTG curves of PLLA, OSF and PLLA/OSF composites thermal degradation at heating rate of 10 °C min^{-1}.

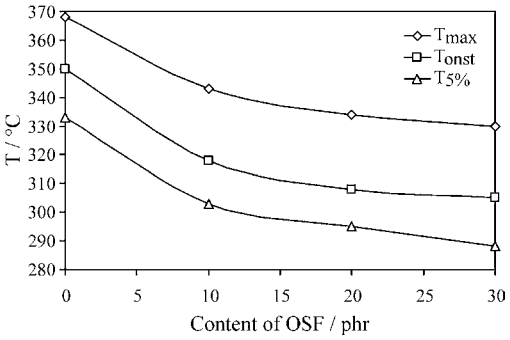

Fig. 7. Influence of OSF content on T_{max}, T_{onst} and $T_{5\%}$ of PLLA at 10 °C min^{-1}.

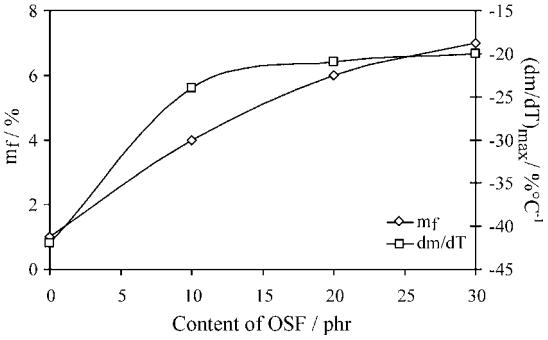

Fig. 8. Influence of OSF content on m_f and $(d\alpha/dt)_{max}$ of PLLA at 10 °C min^{-1}.

stage weight loss of OSF is the evaporation of water and than the decomposition of cellulose, hemicellulose and lignin occurs. The degradation of polysaccharides, hemicellulose and cellulose starts at about 220 and 290 °C, respectively, while lignin degrades around 200 °C [3]. This is in a good agreement with our TG measurements. At higher temperatures lignin appears to be more heat resistant than hemicellulose and cellulose, due to its low degradation rate [3]. Furthermore, lignin is also mainly responsible for the char formation above 400 °C [22]. PLLA/OSF composites decompose in two stages. TG and DTG curves of PLLA/OSF composites at other heating rates have almost the same stages and peaks as at 10 °C/min but more pronounced at lower heating rates. Thermal stability of PLLA decreases as OSF amount increases (Fig. 5). The same behaviour was observed for PLA/wood fibers (WFs) composites by Huda et al. [22]. They concluded that the compatibility and interfacial bonding decreases by mixing of PLLA polymer and WFs. The same can be concluded for PLLA and OSF composites. Addition of OSF broadens the decomposition region and it is wider as OSF amount increases (Fig. 5).

From TG and corresponding DTG curves the onset temperature (T_{onst}), the temperature at 5% weight loss ($T_{5\%}$), the temperature at maximum degradation rate (T_{max}), residual mass of the sample (m_f) and the maximum degradation rate (dm/dT) are obtained (Table 4). From this table is obvious that decomposition of PLLA/OSF composites starts at lower temperatures, at all heating rates, than that of pure PLLA. T_{max} is much lower for the composites as well as $(dm/dT)_{max}$. From m_f values it is evident that the samples were prepared uniformly because variation of m_f for the same sample at different heating rates is minor. m_f for PLLA/OSF composites is in order PLLA 30 > PLLA 20 >PLLA 10, as expected, i.e. higher content of OSF is connected with higher values of residual weight. From Figs. 7 and 8 it is easier to note the trend of influence of OSF on PLLA thermal properties at the heating rate of 10 °C min^{-1}. It is interesting that OSF decelerate thermal degradation of PLLA in an inert, probably due to the char formation and its role as a protective barrier preventing the remain polymer from thermal degradation. Figs. 7 and 8 also shows that OSF content higher than 20 weight parts has no further significant influence on degradation properties of PLLA.

4.3.1. Nonisothermal kinetics analysis

E_a of nonisothermal degradation of PLLA and PLLA/OSF composites were calculated by Friedman method using $\ln(\beta d\alpha/dT)$ versus $1/T$ dependency. Dependence of E_a on α obtained for pure PLLA and

Table 4
TG and DTG data of pure PLLA and PLLA/OSF composites at different heating rates.

Sample	β (°C min^{-1})	T_{onst} (°C)	$T_{5\%}$ (°C)	T_{max} (°C)	m_f (%)	$(dm/dT)_{max}$ (%°C^{-1})
PLLA	2.5	322	304	335	1	13
	5	331	314	349	1	23
	10	350	333	368	1	42
	20	369	352	394	1	54
PLLA 10	2.5	287	277	299	3	7
	5	297	291	320	3	14
	10	318	303	343	4	24
	20	350	323	382	4	47
PLLA 20	2.5	281	268	299	5	7
	5	291	280	309	4	13
	10	308	295	334	6	21
	20	338	308	370	6	46
PLLA 30	2.5	279	262	291	8	8
	5	288	276	310	7	13
	10	305	288	330	7	20
	20	331	303	362	8	44

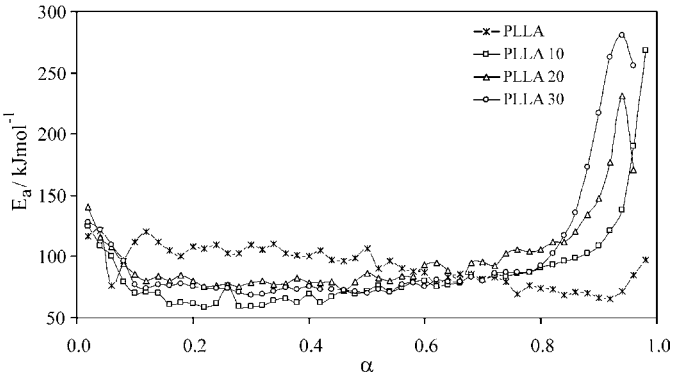

Fig. 9. Activation energy as a function of degree of conversion for pure PLLA and PLLA/OSF composites.

PLLA/OSF composites is presented in Fig. 9. As in all heterogeneous reactions in solid state, E_a calculated in this way is an apparent activation energy. Also, $\alpha < 0.1$ gives unreliable data [23]. In the conversion region from 0.1 to 0.9 the average E_a of nonisothermal degradation of pure PLLA is 93 ± 15 kJ mol^{-1}. The decreasing of E_a in the investigated temperature region as the reaction proceeds is observed. Pure PLLA degrades to low molecular products in low energy consuming process and as degradation proceeds the decrease of E_a is more noticeable. In the literature different values of E_a for pure PLLA degradation can be found, such as 119 ± 4 [7], 110 ($\alpha = 0.01$–0.1) [8], 190–270 (at higher α) [8], 80–160 [19] and 77–132 kJ mol^{-1} (for weight loss 25–90%) [24]. From these values it is clear that E_a is quite different depending probably on different PLLA samples as well as different methods and conversion ranges for calculation. E_a-α curves for PLLA composites could be divided in two regions, first $0.1 < \alpha < 0.8$ and second $\alpha > 0.8$. In the first, wider range of conversions, E_a values for PLLA 10, PLLA 20 and PLLA 30 are 72 ± 9, 85 ± 9 and 77 ± 6 kJ mol^{-1}, respectively. In the second part of E_a-α curve, for $\alpha > 0.8$, E_a of PLLA/OSF composites increases with α due to the char formation and higher E_a needed for degradation. E_a values are in order PLLA 30 > PLLA 20 > PLLA 10. For calculation of other components of kinetic triplet, the defined conversion region ($0.1 < \alpha < 0.8$) as a region of constant E_a can be taken.

5. Conclusions

Biodegradable composites of PLLA and OSF were prepared and the thermal analysis of those materials has been carried out. It was found that OSF promotes the cold crystallization of PLLA. The melting endotherms can be considered as bimodal. Evidently, OSF has the influence on crystallographic form and the morphology of the PLLA crystals as well as on crystallinity degree. PLLA crystallinity is affected by the processing procedure, too. It is assumed that OSF acts as a nucleation agent at lower concentrations but as an obstacle for polymer chains to make crystals at higher concentrations. Introduction of OSF into PLLA has negligible influence on glass transition of PLLA, indicating weak interactions between polymer matrix and the filler. SEM images also show low interfacial adhesion between OSF and PLLA. As the amount of OSF increases the voids and agglomerates of the filler are more visible. TG analysis of the composites at several heating rates shows that addition of OSF deteriorates PLLA thermal stability shifting the beginning of thermal degradation to lower temperatures. Addition of OSF also broadens the degradation region of PLLA and decreases the degradation rate. Amount of OSF higher than 20 weight parts has no further significant influence on degradation properties of PLLA. E_a from nonisothermal data was calculated by Friedman differential isoconversional method. The shape of E_a-α curves revealed that as OSF amount increases the reaction mechanism of PLLA undergoes a quite change. The char formation is probably the main reason of those differences between pure PLLA and PLLA/OSF composites at high degree of conversion.

Acknowledgements

The represented results emerged from the scientific project (Polymer blends with biodegradable components) financially supported by the Ministry of Science, Education and Sports of the Republic of Croatia.

References

[1] H. Tsuji, Polylactides, in: A. Steinbüchel, Y. Doi (Eds.), Biopolymers. Volume 4: Polyesters III – Applications and Commercial Products, Wiley–VCH, Weinheim, 2002, pp. 129–177.
[2] G. Rodríguez, A. Lama, R. Rodríguez, A. Jiménez, R. Guillén, J. Fernández-Bolaños, Bioresour. Technol. 99 (2008) 5261–5269.
[3] V. Tserki, P. Matzinos, S. Kokkou, C. Panayiotou, Compos. Part A 36 (2005) 965–974.
[4] A.P. Mathew, K. Oksman, M. Sain, J. Appl. Polym. Sci. 101 (2006) 300–310.
[5] K. Jamshidi, S.-H. Hyon, Y. Ikada, Polymer 29 (1988) 2229–2234.
[6] A. Sodergard, J.H. Nasman, Polym. Degrad. Stab. 46 (1994) 25–30.
[7] I.C. McNeill, H.A. Leiper, Polym. Degrad. Stab. 11 (1985) 309–326.
[8] F.-D. Kopinke, M. Remmler, K. Mackenzie, M. Milder, O. Wachsen, Polym. Degrad. Stab. 53 (1996) 329–342.
[9] O. Wachsen, K. Platkowski, K.-H. Reichert, Polym. Degrad. Stab. 57 (1997) 87–94.
[10] O. Wachsen, K.H. Reichert, R.P. Kriiger, H. Muchb, G. Schulz, Polym. Degrad. Stab. 55 (1997) 225–231.
[11] J.J.M. Órfão, F.J.A. Antunes, J.L. Figueiredo, Fuel 78 (1999) 349–358.
[12] S. Vyazovkin, N. Sbirrazzuoli, Macromol. Rapid Commun. 27 (2006) 1515–1532.
[13] S. Vyazovkin, C.A. Wight, Annu. Rev. Phys. Chem. 48 (1997) 125–149.
[14] M. Erceg, T. Kovačić, I. Klarić, Conf. Proc. Matrib. (2003) 33–37.
[15] H.L. Friedman, J. Polym. Sci. Part C 6 (1963) 183.
[16] T. Ke, X. Sun, J. Appl. Polym. Sci. 81 (2001) 3069–3082.
[17] S. Pilla, S. Gong, E. O'Neill, L. Yang, R.M. Rowell, J. Appl. Polym. Sci. 111 (2009) 37–47.
[18] B. Andričić, T. Kovačić, S. Perinović, A. Grgić, Macromol. Symp. 263 (2008) 96–101.
[19] Y. Aoyagi, K. Yamashita, Y. Doi, Polym. Degrad. Stab. 76 (2002) 53–59.
[20] I.C. McNeill, H.A. Leiper, Polym. Degrad. Stab. 11 (1985) 267–285.
[21] K. Pielichowski, J. Njuguna, Thermal Degradation of Polymeric Materials, Rapra Technology Limited, Shawbury, 2005.
[22] M.S. Huda, L.T. Drzal, M. Misra, A.K. Mohanty, J. Appl. Polym. Sci. 102 (2006) 4856–4869.
[23] M. Maciejewski, Thermochim. Acta 355 (2000) 145–154.
[24] H. Tsuji, I. Fukui, Polymer 44 (2003) 2891–2896.